8 May 2001

ELSEVIER

Optics Communications 191 (2001) 141–147

OPTICS COMMUNICATIONS

www.elsevier.com/locate/optcom

Concentration of diffuse light at the thermodynamic limit with an aplanatic curved diffractive element

N. Bokor *, R. Shechter, A.A. Friesem, N. Davidson

Department of Physics of Complex Systems, Weizmann Institute of Science, Rehovot 76100, Israel

Received 19 December 2000; accepted 20 February 2001

Abstract

A novel configuration for concentrating diffuse, based on a reflective curved diffractive element, is proposed and demonstrated. Such an aplanatic element satisfies the Abbe sine condition, and hence can achieve diffuse light concentration close to the thermodynamic limit. In our experiments, a thin, cylindrically shaped diffractive element with a numerical aperture of 0.86 yielded a one-dimensional concentration ratio that was 80% of the thermodynamic limit. © 2001 Elsevier Science B.V. All rights reserved.

Keywords: Diffuse light concentration; Curved diffractive elements

1. Introduction

Concentration of diffuse light has many applications including solar energy concentration [1–6], light collection for optical instruments [7–9], efficient light coupling into fiber optics [10]. The amount of concentration is limited to $1/\sin\alpha$ in each transverse dimension, where α is the incoming half-divergence angle. This so-called "thermodynamic limit" arises from the conservation of optical brightness, or étendue [1]. The most widely used non-imaging concentrators, the compound parabolic concentrators approach the thermodynamic limit. However, since their length to width ratio is $\sim 1/\sin\alpha$ [1], they tend to be extremely long for small α. Thus, their use is limited to either highly diffuse beams (large α) or as a secondary stage concentrator, following a first stage concentrator. With the combination of several elements it is possible to considerably reduce the length of non-imaging concentrators [11].

High numerical-aperture (NA) imaging concentrators, in particular those that use simple parabolic mirrors [5], are simpler and more compact than the non-imaging concentrators. However, most imaging concentrators violate the Abbe sine condition, and hence suffer from large first-order aberrations such as comma and astigmatism. These aberrations reduce the concentration ratio far below the thermodynamic limit (for example, by a factor of 2 for one-dimensional and a factor of 4 for two-dimensional parabolic mirrors). Aplanatic imaging systems that obey the Abbe sine condition and hence suppress first-order aberrations, such as microscope objectives, the Luneburg

* Corresponding author. Fax: +972-8-934-4109.

E-mail address: bokor@wisemail.weizmann.ac.il (N. Bokor).

PII: S0030-4018(01)01125-7

lens and the Schmidt camera, are often too complicated and expensive for large area concentrators [1].

In this paper we propose and demonstrate a novel configuration for a diffuse light concentrator, based on a reflective curved diffractive element (CDE). By independently controlling the shape and grating function of the CDE, we found it possible to form a large area concentrator which *exactly* fulfills the Abbe sine condition at extremely high NA [12] and hence concentrates diffuse light at the thermodynamic limit. Experiments with such a CDE, recorded as a simple two-wave interference pattern on a curved surface, yielded much higher concentration than a comparable flat element.

Throughout the paper we resort only to geometrical optics, since for our experiments the diffraction-limited angles and spot sizes are much smaller than the diffusive ones. Moreover, we limit ourselves to quasi-monochromatic diffuse light to suppress the large chromatic aberration of diffractive elements. Finally, we illustrate our approach for a "cylindrical" concentrator that concentrates light in one dimension only. The extension to a "spherical" concentrator that concentrates light in two dimensions is straightforward.

2. Geometrical arrangement

The geometrical arrangements for recording and readout of a cylindrically shaped concentrator are schematically shown in Fig. 1. Fig. 1(a) shows the recording arrangement of the interference of a plane wave and a counter-propagating diverging spherical wave. Fig. 1(b) shows the readout arrangement with a counter-propagating plane wave, where h is the distance of the incoming ray from the optical axis, θ its focusing angle and R is the focal distance which in our case is also the radius of the cylinder. In readout, the first-diffraction-order yields the exact conjugate of the diverging spherical wave and hence a diffraction-limited spot at its origin. Note, that such a diffraction-limited spot would also be obtained when the recording is done on a flat surface. However, only the cylindrical shape [12] exactly fulfills the Abbe sine (or aplanatic) condition [13] of

$$h = R\sin\theta, \quad \text{for all } h < R. \tag{1}$$

The aplanatic condition of Eq. (1) ensures that aberrations which normally grow linearly with the off-axis angle are zero and hence the concentration ratio is expected to be as for ideal imaging, given by

$$\begin{aligned} \mathrm{CR}_{\mathrm{ideal}} &= X_{\mathrm{in}}/X_{\mathrm{out}} = \sin\theta_{\max}/\sin\alpha \\ &= \mathrm{NA}/\sin\alpha, \end{aligned} \tag{2}$$

where X_{in} and X_{out} are the input and output lateral beam sizes, respectively. Note, that as the NA approaches one, Eq. (2) approaches the thermodynamic limit for one-dimensional concentration $\mathrm{CR}_{\max} = 1/\sin\alpha$.

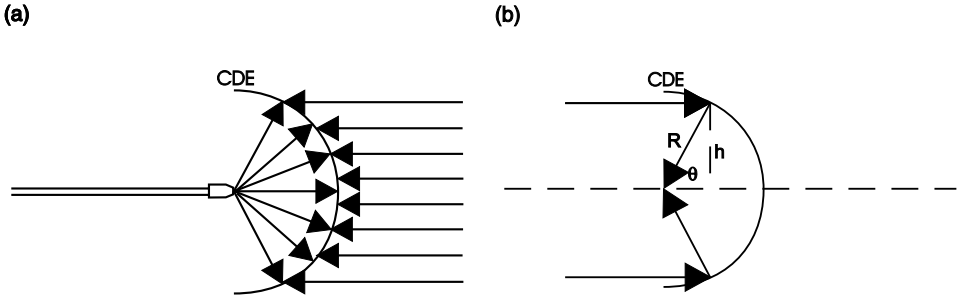

Fig. 1. The geometrical arrangements for recording and readout of a CDE that satisfies the Abbe sine condition: (a) recording geometry; (b) readout geometry.

3. Numerical simulations

To confirm the validity of our approach we calculated, using numerical ray tracing, the normalized concentration ratio (NCR) for the cylindrical CDE as a function of its NA for $R = 3.5$ cm and $\alpha = 1°$ (the same parameters as subsequently used in our experiment). The NCR is defined as $CR/CR_{max} = (X_{in}/X_{out}) \sin\alpha$, where at the thermodynamic limit, NCR = 1. The results are shown in Fig. 2, together with results from two other concentrators: a flat diffractive element (FDE) and a one-dimensional parabolic mirror (Fig. 2 also contains experimental data that will be discussed later). As evident, for high NA, the CDE has the highest concentration ratio, whereas the FDE has the worst one. In particular, the calculated concentration ratio for the CDE is practically indistinguishable from that of the ideal imaging system of Eq. (2), and can approach the thermodynamic limit at high NA. The maximum concentration ratio for the one-dimensional parabolic mirror and the FDE is 50% and 38% of the thermodynamic limit, respectively. Note that the results in Fig. 2 confirm the well-known fact [5] that the highest concentration (50% of the thermodynamic limit) of the one-dimensional parabolic mirror occurs at NA = 0.71, when $\theta_{max} = 45°$. Also note that for three-dimensional concentrators the best concentration ratio for the parabolic mirror and the FDE would be even lower, namely 25% and 14%, respectively, of the thermodynamic limit, whereas for the CDE the thermodynamic limit would still be reached.

The failure of the parabolic concentrator at high NA can be understood by noting that at each point an incident light cone with (half) angle α is reflected as an identical cone towards the focus. However, as the cone intersects the optical axis at an angle θ the focal spot includes an inclination factor $1/\cos\theta$, which diverges for large NA (and reaches an optimum at NA = 0.71 [5]). For the

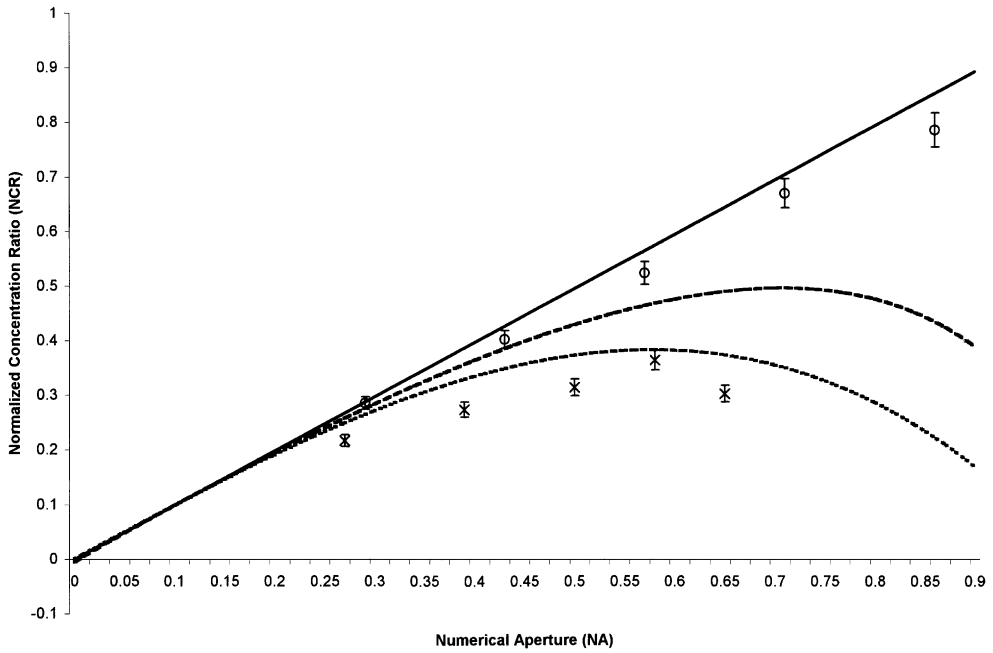

Fig. 2. Calculated NCR as a function of NA for CDE (solid line), FDE (dotted line) and parabolic mirror (dashed line), obtained from ray-tracing analysis. Also shown are the experimental NCR values for CDE (○) and FDE (×). The error bars are estimated from the data.

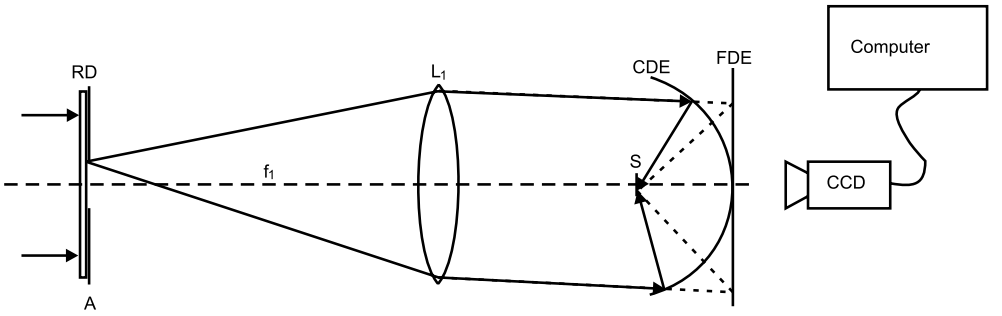

Fig. 3. Setup for measuring the performance of the CDE and FDE.

CDE the reflected light cones for high θ are actually narrower than the incident cones by exactly $\cos\theta$, [1] thereby canceling the effect of the inclination factor $1/\cos\theta$, and yielding identical spot size regardless of the NA (and hence a higher concentration ratio). Finally, the reflected light cone from each point on the FDE is $1/\cos\theta$ times wider than the incident cone, resulting in an even worse concentration.

4. Experiment

For our experiments, we used the arrangement shown in Fig. 1(a) to record a 6 cm wide cylindrical CDE with radius $R = 3.5$ cm and NA $=$ 0.86. A microscope objective of 60×, whose focal point was located exactly at the center of the cylinder was used to generate the spherical wave. The spherical and plane waves were derived from an argon-ion laser operating at a wavelength of 488 nm. The recording material was a 20 μm thick photopolymer which was glued to a thin glass half cylinder. After exposure and development the resulting phase DOE had a diffraction efficiency of ~70%, with uniformity better than ±10% over the entire aperture. For comparison, a FDE was also recorded with the same parameters. The FDE has the same width (6 cm) and focal distance (3.5 cm) as the CDE, but $\mathrm{NA_{FDE}} = \sin(\tan^{-1}(3/3.5)) = 0.65$ is smaller than $\mathrm{NA_{CDE}} = 3/3.5 = 0.86$. Note that by careful control of the recording and development parameters, diffraction efficiencies exceeding 90% can be obtained with photopolymers [14].

The performance of the CDE and FDE concentrators were measured using the setup shown schematically in Fig. 3. The diffuse source was simulated by passing a uniform beam from an argon laser with a wavelength of 488 nm through a rapidly rotating diffuser (RD) located at the back focal length of the lens L_1 (focal distance $f_1 = 56$ cm). An aperture of diameter A was placed adjacent to the RD for controlling the diffusive angle. A horizontal slit of about 1 cm width (not shown in the figure) ensured that our setup is approximately one dimensional (alternatively, we could have replaced the microscope objective during the recording with a cylindrical lens). The focus was obtained on a 5 mm wide screen (S) located at the focal plane of the CDE or FDE, and imaged onto a calibrated CCD camera and digitized to a computer. The resolution of the entire system (concentrator + diagnostics imaging and CCD pixel resolution) was measured to be better than 0.1 mm by setting the diameter of the aperture to $A < 1$ mm. Next by setting $A = 20$ mm, we obtained a diffuse (half) angle of $\alpha = A/2f_1 = 1°$ (much smaller than the Bragg-selectivity angle of the CDE and FDE, to ensure high diffraction efficiency).

Some representative experimental concentrated spots for the CDE and FDE are shown in Fig. 4. The relevant parameters for the results were the following: element aperture = 6 cm, focal length

[1] Remark: this surprising result is directly obtained from the diffraction relations of the grating for small α, and is an excellent approximation even for large α.

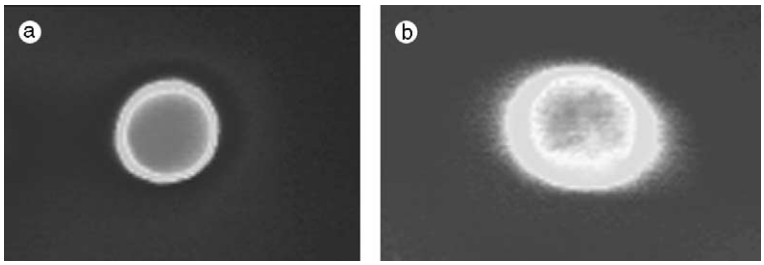

Fig. 4. Experimental concentrated spots (a) with CDE; (b) with FDE. Element aperture = 6 cm, $R = 3.5$ cm and $\alpha = 1°$.

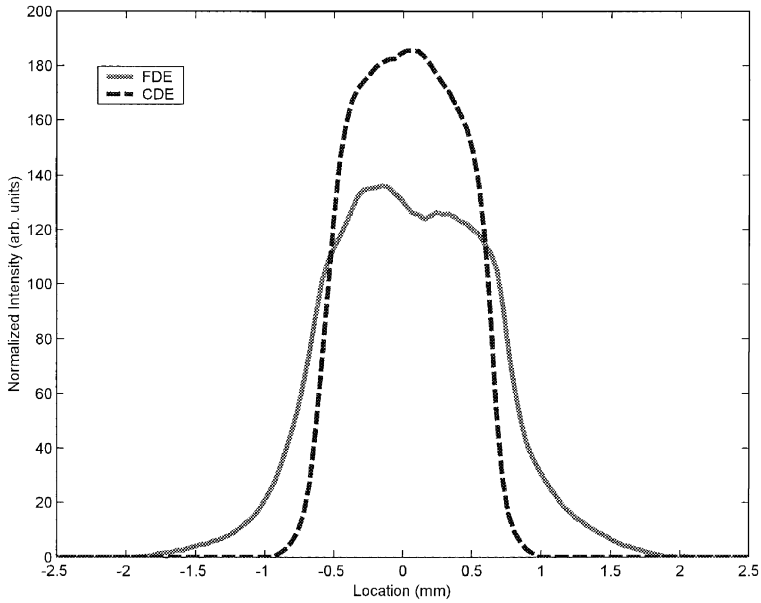

Fig. 5. Measured intensity cross-sections of the concentrated spots of Fig. 4; CDE (dashed line) and FDE (solid line).

$R = 3.5$ cm and $\alpha = 1°$. The corresponding intensity cross-sections are shown in Fig. 5. As evident, the CDE yielded a narrower spot than the FDE, with clearly observable sharper edges. The results for the corresponding calculated intensity cross-sections – obtained from numerical ray tracing – are presented in Fig. 6. They reveal a very good agreement with the experimental results. In particular, the measured ratio of peak intensity of the concentrated spot by the CDE to that concentrated by the FDE is 1.36, very close to the calculated ratio of 1.42. We repeated these measurements as a function of the NA for the CDE and FDE. For these measurements we varied the width of an aperture placed adjacent to the elements in order to limit their effective width. The experimental results are shown in Fig. 2. As evident, the experimental results agree quite well with the calculated results for both the CDE and FDE. They confirm the superiority of the CDE over the FDE, especially at high NAs. Specifically, the maximal NCR for the CDE was 0.79 at NA of 0.86, whereas that for the FDE was only 0.37 at NA of 0.58.

5. Conclusion

To conclude, we proposed and demonstrated an aplanatic imaging concentrator based on a thin

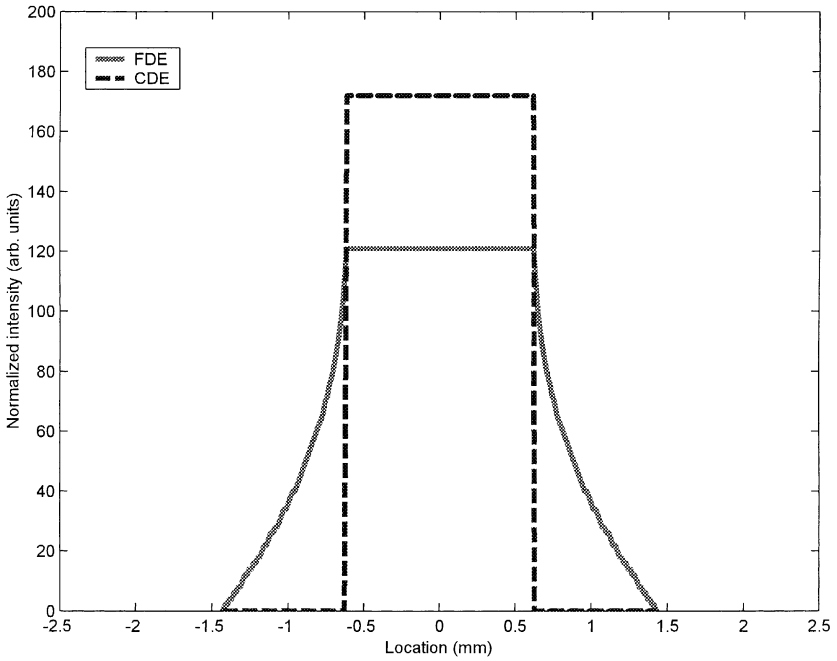

Fig. 6. Calculated intensity cross-sections of the concentrated spots with the same parameters used to obtain the results in Fig. 5; CDE (dashed line) and FDE (solid line).

diffractive element with a cylindrical shape, that allows concentration at the thermodynamic limit. Our experimental results verified nearly ideal concentration for a large (6 cm diameter) element up to the maximal NA of 0.86 we could record. CDEs with even higher NA can be of course recorded by resorting to either stronger microscope objectives or several exposures of the same two beam interference pattern while rotating the element around the center of the cylinder. We estimate that using two exposures with the same 60× objective we used, NA = 1 can be obtained. Such an element can achieve concentration at the thermodynamic limit. Such relatively simple recording arrangements could be extended to very large scale, whereby the quality of concentration depends only weakly on the exact shape of the CDE, as long as it is identical during recording and readout. Finally, the approach can be readily extended to spherical concentrators that concentrate light in two directions by simply using a thin CDE, shaped as a spherical surface. This can be done by dip-coating photopolymer, photoresist or dichromated gelatin on thin half-spherical substrates.

References

[1] R. Winston, W.T. Welford, High Collection Nonimaging Optics, Academic, New York, 1989.
[2] I.M. Bassett, W.T. Welford, R. Winston, Nonimaging optics for flux concentration, in: E. Wolf (Ed.), Progress in Optics, vol. 27, North-Holland, Amsterdam, 1989, pp. 161–226.
[3] I. Pe'er, N. Naftali, A. Yogev, High-power solar-pumped Nd:YAG laser amplifier for free-space laser communication, in: R. Winston (Ed.), Nonimaging Optics: Maximum Efficiency Light Transfer IV, Proceedings of SPIE 3139, 1997, pp. 194–204.
[4] M. Brunotte, A. Goetzberger, U. Blieske, Two-stage concentrator permitting concentration factors up to 300× with one-axis tracing, Solar Energy 56 (1996) 285–300.
[5] N. Davidson, L. Khaykovich, E. Hasman, Anamorphic concentration of solar radiation beyond the one-dimensional thermodynamic limit, Appl. Opt. 39 (2000) 3963–3967.

[6] N. Davidson, A.A. Friesem, One dimensional concentration of diffuse light, Opt. Commun. 99 (1993) 162–166.
[7] N. Davidson, L. Khaykovich, E. Hasman, High-resolution spectrometers for diffuse light using anamorphic concentration, Opt. Lett. 24 (1999) 1835–1837.
[8] S. Yamaguchi, T. Kobayashi, Y. Sainto, K. Chiba, Collimation of emissions from a high-power multistripe laser-diode bar with multiprism array coupling and focusing to a small spot, Opt. Lett. 20 (1995) 898–900.
[9] N. Davidson, A.A. Friesem, Concentration and collimation of diffuse linear light sources, Appl. Phys. Lett. 62 (4) (1993) 334–336.
[10] H. Zbinden, J.E. Balmer, Q-switched Nd:YLF laser end pumped by a diode-laser bar, Opt. Lett. 15 (1990) 1014–1016.
[11] J.C. Miñano, J.C. González, New method of design of nonimaging concentrators, Apt. Opt. 31 (1992) 3051–3060.
[12] W.T. Welford, Aplanatic hologram lenses on spherical surfaces, Opt. Commun. 9 (3) (1973) 268–269.
[13] M.V. Klein, T.E. Furtak, Optics, Wiley, New York, 1986.
[14] V. Weiss, E. Millul, A.A. Friesem, Photopolymeric holographic recording media: in-situ and real-time characterization, Proc. SPIE 2688 (1996) 11–20.